

Analytically Approximation Solution to Higher Derivative Gravity

S. N. Sajadi*, Robert B. Mann†, N. Riazi‡, Saeed Fakhry§

Department of Physics, Shahid Beheshti University, G.C., Evin, Tehran 19839, Iran

Physics Department and Biruni Observatory, College of Sciences, Shiraz University, Shiraz 71454, Iran

Department of Physics and Astronomy, University of Waterloo, Waterloo, Ontario, Canada N2L 3G1

October 29, 2020

Abstract

We obtain analytical approximate black hole solutions for higher derivative gravity in the presence of Maxwell electromagnetic source. We construct near horizon and asymptotic solutions and then use these to obtain an approximate analytic solution using a continued fraction method to get a complete solution. We compute the thermodynamic quantities and check the first law and Smarr formula. Finally, we investigate the null and time-like geodesics of this black hole.

1 Introduction

Einstein's general relativity is a remarkably successful theory of gravity. By predicting and describing new fundamental phenomena such as black holes, gravitational waves and cosmic expansion, it has become a cornerstone of modern theoretical physics and astronomy. Recently, some of its predictions have been confirmed by the direct detection of black hole and its shadow and gravitational waves from binary black hole merger.

Despite such enormous successes, it has some limitations. As a classical field theory, it does not take quantum effects into account. In order to understand them, with an ultimate vision to unify general relativity with quantum theory, it is necessary to go beyond general relativity. In effective field theories, Einstein gravity is extended by higher-order terms in curvature that represent quantum corrections that emerge from high energy regimes. If one adds all possible quadratic curvature invariants to the usual Einstein-Hilbert action one obtains a theory free of ultraviolet divergences [1]. However the linearized equations of motion of these theories allow unphysical ghost-like modes [2]. Although such ghosts in general violate unitarity, and thus the probabilistic interpretation of quantum theory, there are some arguments [3] indicating that this is not a severe problem. In this case there are some theories that lead to ghosts [4]. The details of this renormalization have been discussed elsewhere [2] and will not be considered here.

We consider here the search for electric charged black hole solutions in Einstein Quadratic Gravity, which is general relativity extended by quadratic curvature invariants in the action.

*Electronic address: naseh.sajadi@gmail.com

†Electronic address: rbmann@uwaterloo.ca

‡Electronic address: n_riazi@sbu.ac.ir

§Electronic address: s_fakhry@sbu.ac.ir

Black holes are fundamental objects in a theory of gravity, providing powerful probes for studying subtle aspects of a theory of gravity. In addition to the Schwarzschild solution, there is another spherically symmetric asymptotically flat non Schwarzschild black hole solution within the same theory that admits positive and negative values for the black hole mass [5]. The search for new electrically charged black hole solutions, has been carried out numerically [6]. However numerical solutions do not give a clear picture of the metric dependence on physical parameters of the system. We therefore seek an analytic method to obtain a highly accurate analytic approximate solution to the field equations.

To this end we employ a continued fraction expansion ansatz [7]. This ansatz is designed so that the coefficients in the continued fraction are fixed by behaviour of the metric near the event horizon, while the pre-factors are introduced to match the asymptotic behaviour at infinity. This way an accurate analytic expression approximating the metric can be obtained for the whole space outside the event horizon, and not only near the black hole or far from it. The continued fraction approximation is not only useful for the present analysis, but also, proves useful in concerning quasi-normal modes [8]. With the continued fraction solution in hand, we study the properties of the black hole solution. Specifically we analyze the motion of particles around the black hole, constraining the coupling with solar system tests, and investigating the properties of its shadow. We exhibit constraints on the coupling constant α of the theory by using Shapiro time delay. We find that the theory can be compatible with solar system tests whilst maintaining relatively large values of the coupling. Furthermore, we find that the radius of the innermost stable circular orbit around the black hole and the angular momentum of a test body at this radius increase with increasing α as compared to their corresponding values in general relativity.

Our paper is organized as follows. In the next section we review the near horizon and asymptotic solutions. Then, using a continued fraction expansion, we obtain an approximate analytic solution from the first law thermodynamics and Smarr formula. In Sec. 3 we study some properties of the black holes and investigate the orbit of particles around it. we constrain the coupling constant by using Shapiro test in solar system. Finally, in sec. 4 we present our conclusions.

2 Basic equations

The most general Lagrangian with electromagnetic field and the cosmological constant Λ can be written as

$$L = \gamma(R - 2\Lambda) - \alpha C_{abcd}C^{abcd} + \beta R^2 - \kappa F_{ab}F^{ab} \quad (1)$$

where F_{ab} is the electromagnetic tensor and C_{abcd} is the Weyl tensor, α , β , γ and κ are coupling constants. Since the trace of the equations of motion in the absence of a cosmological constant vanishes, the term proportional to β does not contribute to the solution. Henceforth we set $\beta = 0$, and for simplicity we also set $\gamma = \kappa = 1$ [5].

The field equations are then given by

$$E_{ab} = R_{ab} - \frac{1}{2}g_{ab}R - \Lambda g_{ab} - 4\alpha B_{ab} - 2T_{ab} = 0 \quad , \quad \nabla_a F^{ab} = 0 \quad (2)$$

where T_{ab} and B_{ab} are

$$B_{ab} = \left(\nabla^m \nabla^n + \frac{1}{2}R^{mn} \right) C_{ambn} \quad , \quad T_{ab} = F_{da}F^d{}_b - \frac{1}{4}g_{ab}F_{de}F^{de}. \quad (3)$$

We consider following static, spherical symmetric metric

$$dS^2 = -h(r)dt^2 + \frac{dr^2}{f(r)} + r^2 \left(d\theta^2 + \frac{\sin^2(\sqrt{k}\theta)}{k} d\phi^2 \right). \quad (4)$$

By inserting the metric into the field equations we obtain the differential equations for $f(r)$ and $h(r)$, with

$$R + 4\Lambda = -2fhr^2h'' + fr^2h'^2 - rhh'(rf' + 4f) + 4h^2(2\Lambda r^2 - rf' + k - f) = 0, \quad (5)$$

from taking the trace (where the prime denotes the r derivative), with

$$\begin{aligned} E_{rr} - 2T_{rr} = & \\ & \left(-6\alpha h^2 fr^3 h' + 12r^2 \alpha h^3 f\right) f'' + \left(12\alpha h^3 rk - 3\alpha h fr^3 h'^2 - 12\alpha h^3 fr - 6\alpha h^2 fr^2 h' + 24\alpha h^3 r^3 \Lambda\right) f' \\ & - 9\alpha h^3 r^2 f'^2 + \left(16\alpha h^3 \Lambda r^2 + 6h^3 r^2 + 6r^3 h^2 h' + 24\alpha kh^3 + 6q^2 h^2 + 16\alpha r^3 h^2 h' \Lambda\right) f \\ & + \left(-9\alpha hr^2 h'^2 - 24\alpha h^3 + 3\alpha r^3 h'^3\right) f^2 + \left((-16\alpha \Lambda^2 - 6\Lambda)r^2 - 6k - 16\alpha k\Lambda\right) r^2 h^3 = 0 \end{aligned} \quad (6)$$

being the only other non-redundant field equation. Expanding the functions $h(r)$ and $f(r)$ around the event horizon r_+

$$h(r) = h_1(r - r_+) + h_2(r - r_+)^2 + h_3(r - r_+)^3 + \dots \quad (7)$$

$$f(r) = f_1(r - r_+) + f_2(r - r_+)^2 + f_3(r - r_+)^3 + \dots \quad (8)$$

and then inserting these expressions into equations (5) and (6), we find

$$h_2 = \frac{r_+ h_1 \Lambda^2}{3f_1^2} + \left(\frac{5h_1}{3f_1} + \frac{kh_1}{3r_+ f_1^2} + \frac{r_+ h_1}{8\alpha f_1^2}\right) \Lambda + \frac{kh_1 - 2f_1 h_1 r_+}{f_1 r_+^2} + \frac{kh_1 r_+^2 - f_1 h_1 r_+^3 - q^2 f_1}{8\alpha f_1^2 r_+^3}, \quad (9)$$

and

$$f_2 = -\frac{r_+ \Lambda^2}{f_1} + \left(3 - \frac{k}{r_+ f_1} - \frac{3r_+}{8\alpha f_1}\right) \Lambda + \frac{k - 2f_1 r_+}{r_+^2} - \frac{3(kh_1 r_+^2 - f_1 h_1 r_+^3 - q^2 f_1)}{8\alpha f_1 h_1 r_+^3} \quad (10)$$

where r_+ and f_1 are undetermined constants of integration. The parameter h_1 can be absorbed into the definition of the t coordinate in the near-horizon expansion; however doing so would have implications for the large- r and continued fraction solutions we shall obtain, and so we have retained it in the above. For $q = 0$ this solution reduces to the near-horizon solution obtained previously [5] for the theory given in (1). We also note the existence of an alternate solution whose near-horizon expansion has a well-defined small- α limit – we discuss this in Appendix B.

All higher-order coefficients in (7) and (8) are determined in terms of these quantities and r_+ (and the coupling parameters); we provide expressions for the higher-order coefficients in the Appendix.

To obtain a solution for $h(r)$ and $f(r)$ at large r , we write

$$h(r) = 1 + \varepsilon \mathcal{H}(r) + \mathcal{O}(\varepsilon^2), \quad f(r) = 1 + \varepsilon \mathcal{F}(r) + \mathcal{O}(\varepsilon^2) \quad (11)$$

where $\varepsilon \ll 1$. Substituting Eqs. (11) into Eqs. (5) and (6) the field equations become

$$2\alpha r^2 \mathcal{F}'' + r^3 \mathcal{H}' + r^2 \mathcal{F} - 4\alpha \mathcal{F} + q^2 = 0, \quad (12)$$

$$\frac{1}{2} r^2 \mathcal{H}'' + r \mathcal{H}' + r \mathcal{F}' + \mathcal{F} = 0, \quad (13)$$

to order ε . Solving for \mathcal{H}' from Eq. (12)

$$\mathcal{H}' = -\frac{2\alpha}{r} \mathcal{F}'' - \left(1 - \frac{4\alpha}{r^2}\right) \frac{\mathcal{F}}{r} - \frac{q^2}{r^3} \quad (14)$$

and inserted this into (13) yields

$$-2\alpha r \mathcal{F}''' - 2\alpha \mathcal{F}'' + \left(r + \frac{4\alpha}{r}\right) \mathcal{F}' + \left(1 - \frac{4\alpha}{r^2}\right) \mathcal{F} = -\frac{q^2}{r^2}, \quad (15)$$

The corresponding homogenous equation is

$$-2\alpha r \mathcal{F}_g''' - 2\alpha \mathcal{F}_g'' + \left(r + \frac{4\alpha}{r}\right) \mathcal{F}_g' + \left(1 - \frac{4\alpha}{r^2}\right) \mathcal{F}_g = 0 \quad (16)$$

whose solution is

$$\mathcal{F}_g = \frac{C_1}{r} + \frac{C_2(\sqrt{2\alpha} + r)e^{-\frac{r}{\sqrt{2\alpha}}}}{r} - \frac{C_3(-\sqrt{2\alpha} + r)e^{\frac{r}{\sqrt{2\alpha}}}}{r}. \quad (17)$$

This solution consists of a growing mode and a decaying mode. Asymptotic flatness demands that we set $C_3 = 0$ [24] and the constant C_1 can be interpreted as the black hole's mass ($C_1 = -2M$). The second term decays exponentially and one can therefore be neglected.

The particular solution to (15) can be obtained using the ansatz

$$\mathcal{F}_s = \sum_{n=2} \frac{F_n}{r^n}, \quad (18)$$

from which we find

$$\mathcal{F}_s = \frac{q^2}{r^2} + \frac{8\alpha q^2}{r^4} + \frac{288\alpha^2 q^2}{r^6} + \frac{23040\alpha^3 q^2}{r^8} + \dots \quad (19)$$

yielding

$$f(r) = 1 + \varepsilon(\mathcal{F}_g + \mathcal{F}_s) = 1 - \frac{2M}{r} + \frac{q^2}{r^2} + \frac{8\alpha q^2}{r^4} + \frac{288\alpha^2 q^2}{r^6} + \frac{23040\alpha^3 q^2}{r^8} + \dots \quad (20)$$

as the solution for $f(r)$, neglecting the exponentially decaying terms. Inserting this into (14), we get

$$h(r) = 1 - \frac{2M}{r} + \frac{q^2 - 2\alpha}{r^2} + \frac{4\alpha q^2}{r^4} + \frac{96\alpha^2 q^2}{r^6} + \frac{5760\alpha^3 q^2}{r^8} + \dots \quad (21)$$

where we have set¹ $\varepsilon = 1$.

We wish to obtain an approximate analytic solution (for $k = 1$) that is valid near the horizon and at large r . To this end we employ a continued fraction expansion [11], and write

$$h(r) = xA(x), \quad \frac{h(r)}{f(r)} = B^2(x), \quad (22)$$

with

$$A(x) = 1 - \epsilon(1 - x) + (a_0 - \epsilon)(1 - x)^2 + \tilde{A}(x)(1 - x)^3 \quad (23)$$

$$B(x) = 1 + b_0(1 - x) + \tilde{B}(x)(1 - x)^2 \quad (24)$$

¹We note that our asymptotic expansions (20,21) do not agree with those obtained previously [6] for the charged case.

where

$$x = 1 - \frac{r_+}{r} \quad \tilde{A}(x) = \frac{a_1}{1 + \frac{a_2 x}{1 + \frac{a_3 x}{1 + \frac{a_4 x}{1 + \dots}}}} \quad \tilde{B}(x) = \frac{b_1}{1 + \frac{b_2 x}{1 + \frac{b_3 x}{1 + \frac{b_4 x}{1 + \dots}}} \quad (25)$$

where we truncate the continued fraction at order 4. By expanding (22) near the horizon ($x \rightarrow 0$) and the asymptotic region ($x \rightarrow 1$) we obtain

$$\epsilon = -\frac{H_1}{r_+} - 1, \quad b_0 = 0, \quad a_0 = \frac{q^2 - 2\alpha}{r_+^2} \quad (26)$$

for the lowest order expansion coefficients, with the remaining a_i and b_i given in terms of (r_+, q, h_1, f_1) ; we provide these expressions in the Appendix.

The resultant expressions are somewhat cumbersome to deal with, so henceforth we set $f_1 = h_1$ for the sake of simplicity. This yields a more restricted set of solutions that still capture the basic physics of the higher-curvature effects. Note that this restriction does not imply that $f(r) = h(r)$.

The result is an approximate analytic solution for both metric functions everywhere outside the horizon. In Figures (1)-(2) we present the solutions for $f(r)$ and $h(r)$, depicting the full continued fraction solution (22) along with its comparison to the near-horizon and large- r series expansions, the latter given by dot-dashed lines. We see that the continued fraction expansion converges to both of these other approximations.

We find two groups of solutions. One group reduces to the Reissner-Nordstrom as $\alpha \rightarrow 0$ – these are charged generalizations of the uncharged case studied previously [5]. This group of solutions is shown in Figure 1 for three different values of q . The metric functions are increasing functions in $r \geq r_+$.

Figure 2 illustrates the second group of solutions for the same values of q . These solutions are physically distinct from the first group, having a peak outside of the event horizon. This peak is related to a negative mass [5] for the black hole. For a static space time we have a timelike Killing vector $\xi = \partial_t$ everywhere outside the horizon and so we obtain

$$T = \frac{1}{4\pi} \sqrt{\frac{f(r_+)}{h(r_+)}} h'(r) \Big|_{r_+} = \frac{f_1}{4\pi} = \frac{(1 - 2\epsilon + a_1 + a_0)}{4\pi r_+ (1 + b_1)} = \frac{(1 + \delta(r_+, q))}{4\pi r_+} \quad (27)$$

for the temperature T , where we have defined $f_1 = \frac{1 + \delta}{r_+}$. We find in (68) that b_1 has two values, which are $b_1 = b_1^- = 0$ and $b_1 = b_1^+ = -2$ for $f_1 = h_1$. We shall only consider the first of these, as the second one leads to negative temperature.

Extreme charged black hole solutions exist if $f_1 = 0$, implying that $a_1 = 2\epsilon - 1 - a_0$ and so $h_1 = 0$. We then must also have $q^2 = r_+^2$ in order that the remaining parameters in (7) and (8) are finite. The mass for this branch of solutions is not always positive [5].

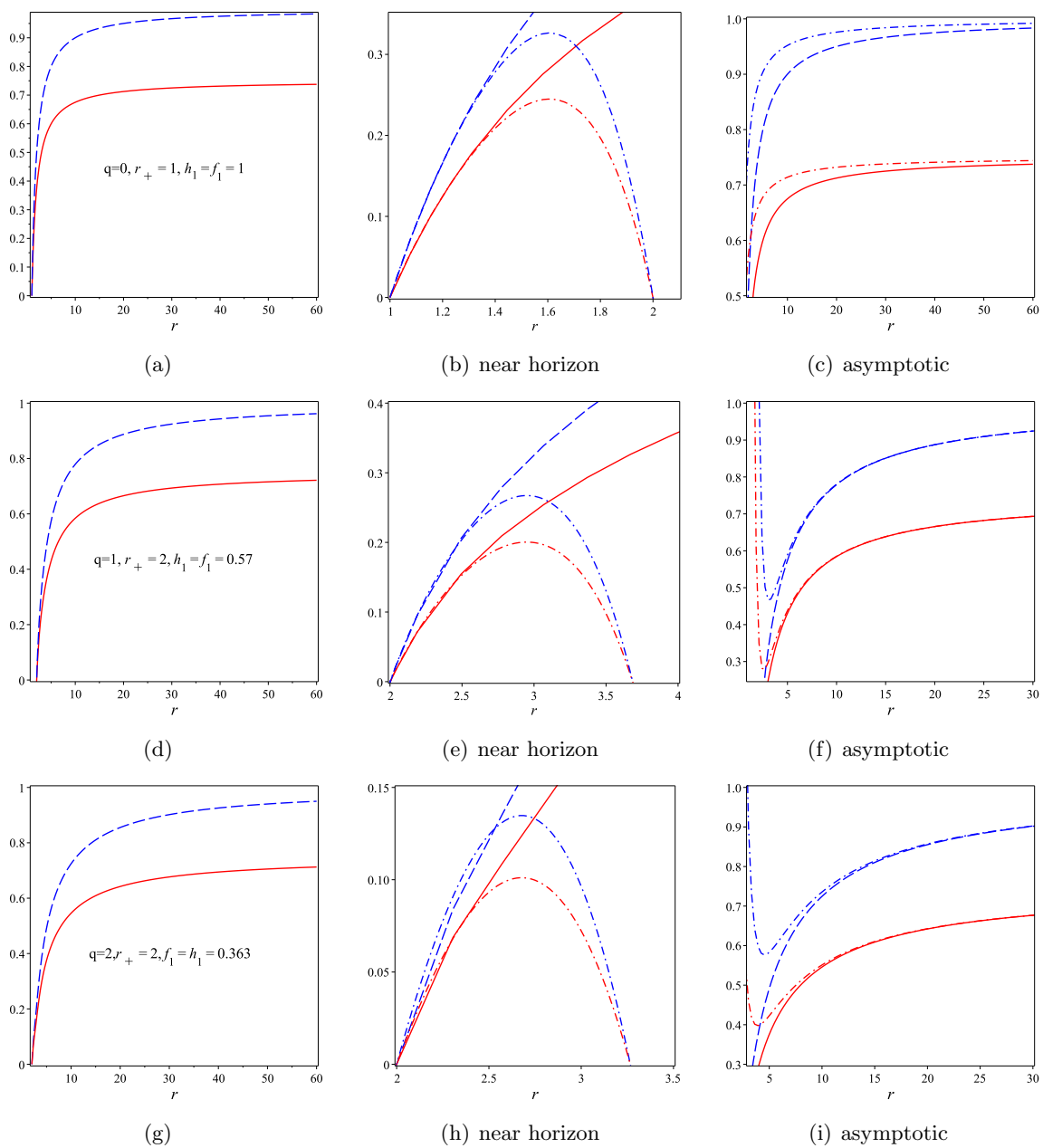


Figure 1: The behavior of $f(r)$ (blue dashed line) and $0.75h(r)$ (red solid line) in terms of r for $k = 1, \alpha = 0.5$, for the first group of solutions. The top row is $q = 0$, the middle row $q = 1$, and the bottom row $q = 2$. The left column is the full continued fraction solution, the middle column compares this solution to the near-horizon approximation (dot-dashed lines), and that right column compares this solution to the large- r approximation (dot-dashed lines). All dimensional quantities are in units of M .

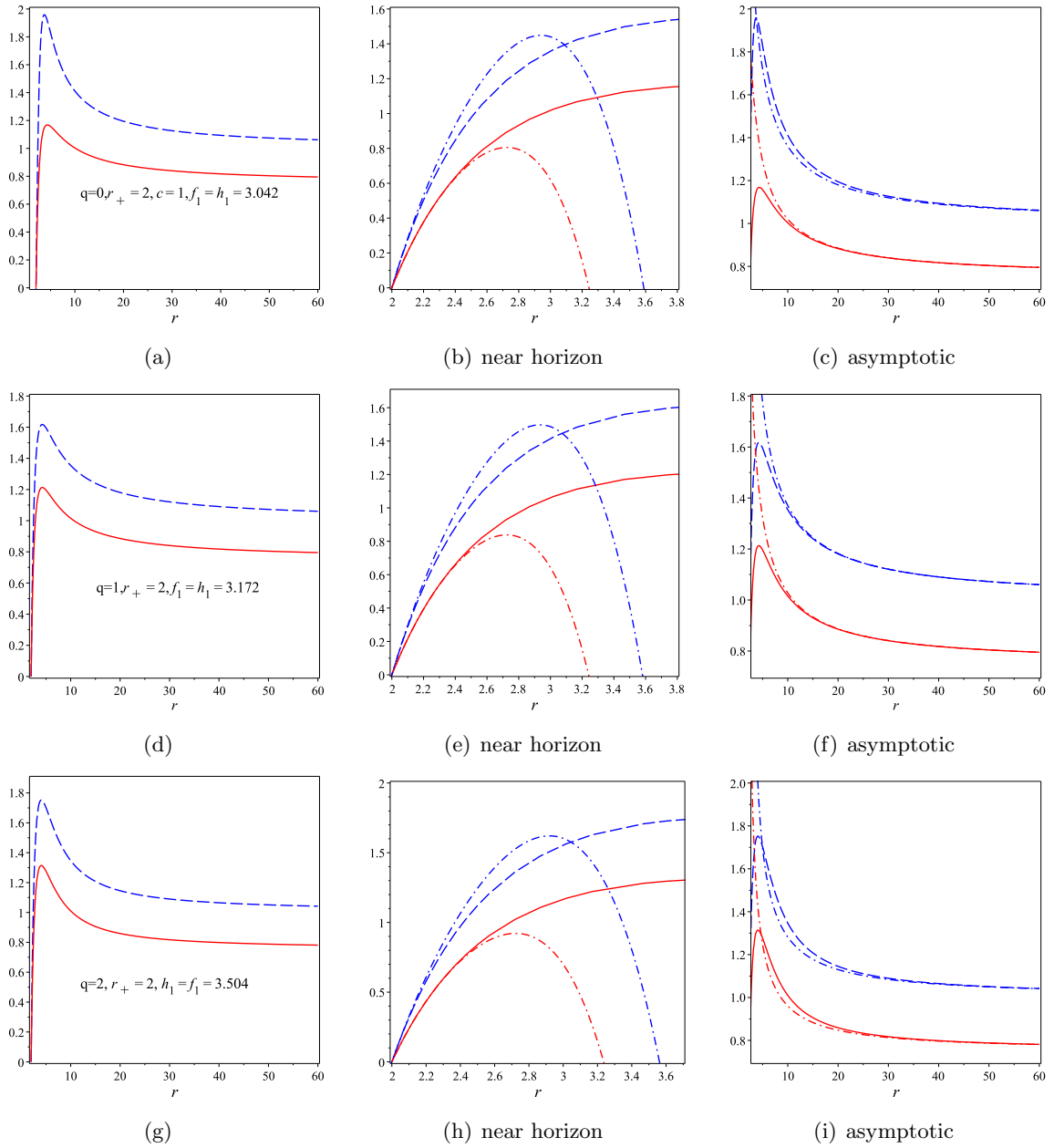


Figure 2: The behavior of $f(r)$ (blue dashed line) and $0.75h(r)$ (red solid line) in terms of r for $k = 1, \alpha = 0.5$, for the second group of solutions. The top row is $q = 0$, the middle row $q = 1$, and the bottom row $q = 2$. The left column is the full continued fraction solution, the middle column compares this solution to the near-horizon approximation (dot-dashed lines), and that right column compares this solution to the large- r approximation (dot-dashed lines). All dimensional quantities are in units of M .

We compute the entropy as follows [16, 17, 18]

$$\begin{aligned} S &= -2\pi \int_{Horizon} d^2x \sqrt{\eta} \frac{\delta L}{\delta R_{abcd}} \epsilon_{ab} \epsilon_{cd} = \frac{A}{4} \left[1 + 4\alpha \left(\frac{1}{r_+^2} - \frac{f'(r_+)}{r_+} \right) \right] = \frac{A}{4} \left(1 + \frac{4\alpha}{r_+^2} (1 - r_+ f_1) \right) \\ &= \frac{A}{4} \left(1 - \frac{4\alpha \delta(r_+, q)}{r_+^2} \right) \end{aligned} \quad (28)$$

where our choice $f_1 = h_1$ implies $b_1 = 0$ (as is clear from (68) in Appendix A), leading to $B = 1$ in (24). We see that if $\delta(r_+, q) > 0$ then $\frac{4S}{A} < 1$.

The electric potential is

$$\phi = \int_{r_+}^{\infty} \frac{Bq}{r^2} dr = \frac{q}{r_+} \quad (29)$$

We now consider the thermodynamics of these black hole solutions, whose basic equations are the first law and Smarr formula

$$dM = TdS + \phi dq \quad (30)$$

$$M = 2TS + q\phi \quad (31)$$

where there are no pressure/volume terms since we have set $\Lambda = 0$. From Eq. (31) we have

$$M = \frac{(1 + \delta(r_+, q))r_+}{2} - \frac{2\alpha(1 + \delta(r_+, q))\delta(r_+, q)}{r_+} + \frac{q^2}{r_+} \quad (32)$$

yielding the mass parameter as a function of the horizon radius and the charge.

We now impose the first law (30), which becomes

$$\frac{\partial M}{\partial r_+} dr_+ + \frac{\partial M}{\partial q} dq = T \frac{\partial S}{\partial r_+} dr_+ + T \frac{\partial S}{\partial q} dq + \phi dq \quad (33)$$

yielding

$$\begin{aligned} \frac{\partial M}{\partial r_+} - T \frac{\partial S}{\partial r_+} &= 0, \quad \implies \\ \left[\frac{r_+}{2} - \frac{\alpha}{r_+} \right] \frac{\partial \delta(r_+, q)}{\partial r_+} + \frac{\alpha \delta(r_+, q)}{r_+} \left[-\frac{3\partial \delta(r_+, q)}{\partial r_+} + \frac{2}{r_+} + \frac{2\delta(r_+, q)}{r_+} \right] - \frac{q^2}{r_+^2} &= 0 \end{aligned} \quad (34)$$

and

$$\frac{\partial M}{\partial q} - T \frac{\partial S}{\partial q} - \phi = 0, \quad \implies \left[\frac{r_+}{2} - \frac{\alpha}{r_+} \right] \frac{\partial \delta(r_+, q)}{\partial q} - \frac{3\alpha}{r_+} \delta(r_+, q) \frac{\partial \delta(r_+, q)}{\partial q} + \frac{q}{r_+} = 0. \quad (35)$$

as differential equations that must be satisfied by $\delta(r_+, q)$.

Consider first the neutral case $q = 0$. Equation (34) yields

$$-\frac{(r_+^2 - 2\alpha)\delta(r_+)(1 + \delta(r_+))^2}{3r_+^2} + \frac{\delta(r_+)^3}{3} + \frac{\delta(r_+)^2}{2} + \frac{K - 1}{6} = 0. \quad (36)$$

As can be seen, the equation (36) is cubic and there is at least one root for δ depends to the sign of the discriminant Δ . The discriminant for cubic equation (36) is

$$\Delta = \frac{K(r_+^6 + 12\alpha r_+^4 + \alpha^2(48K - 108)r_+^2 + 64\alpha^3)}{324r_+^6}. \quad (37)$$

for positive values of α and K , for large and small r_+ the discriminant is positive which means there are three roots. There will be an intermediate range of r_+ where equation (37) depending on the values of K and α could go negative. as an algebraic equation for $\delta(r_+)$, with K a constant of integration and (36) trivially satisfied. Solving this yields

$$\delta_1(r_+) = A + \frac{(r_+^2 + 4\alpha)^2}{144\alpha^2 A} + \frac{r_+^2 - 8\alpha}{12\alpha} \quad (38)$$

$$\delta_2(r_+) = \frac{-(1 - \sqrt{3}i)A}{2} + \frac{r_+^2 - 8\alpha}{12\alpha} - \frac{(r_+^2 + 4\alpha)^2(1 + \sqrt{3}i)}{288\alpha^2 A} \quad (39)$$

$$\delta_3(r_+) = \frac{-(1 + \sqrt{3}i)A}{2} + \frac{r_+^2 - 8\alpha}{12\alpha} + \frac{(r_+^2 + 4\alpha)^2(\sqrt{3}i - 1)}{288\alpha^2 A} \quad (40)$$

where

$A =$

$$\frac{\left(r_+^6 + 12\alpha r_+^4 + 64\alpha^3 - 24(9K - 2)\alpha^2 r_+^2 + 12\sqrt{3}\alpha r_+ \sqrt{K(12\alpha^2 r_+^2(9K - 4) - (r_+^6 + 12\alpha r_+^4 + 64\alpha^3))}\right)^{\frac{1}{3}}}{12\alpha} \quad (41)$$

For different values of K , the discriminant and the roots have been shown in Fig. 3. As can be seen, from Fig. 3 for $K \leq 1$, Δ for all values of r_+ is positive. This shows there are three real solution for δ which have been depicted in Fig. 3(b, d, f). For $K = 1.1$, Δ in small r_+ becomes negative which leads to a solution for δ as shown in Fig. 3f. In Fig. 3d, δ for the dashed line curves vanishes which is corresponds to the Schwarzschild-like behaviour. Any deviation from this line (solid lines) corresponds to the non- Schwarzschild-like behaviour.

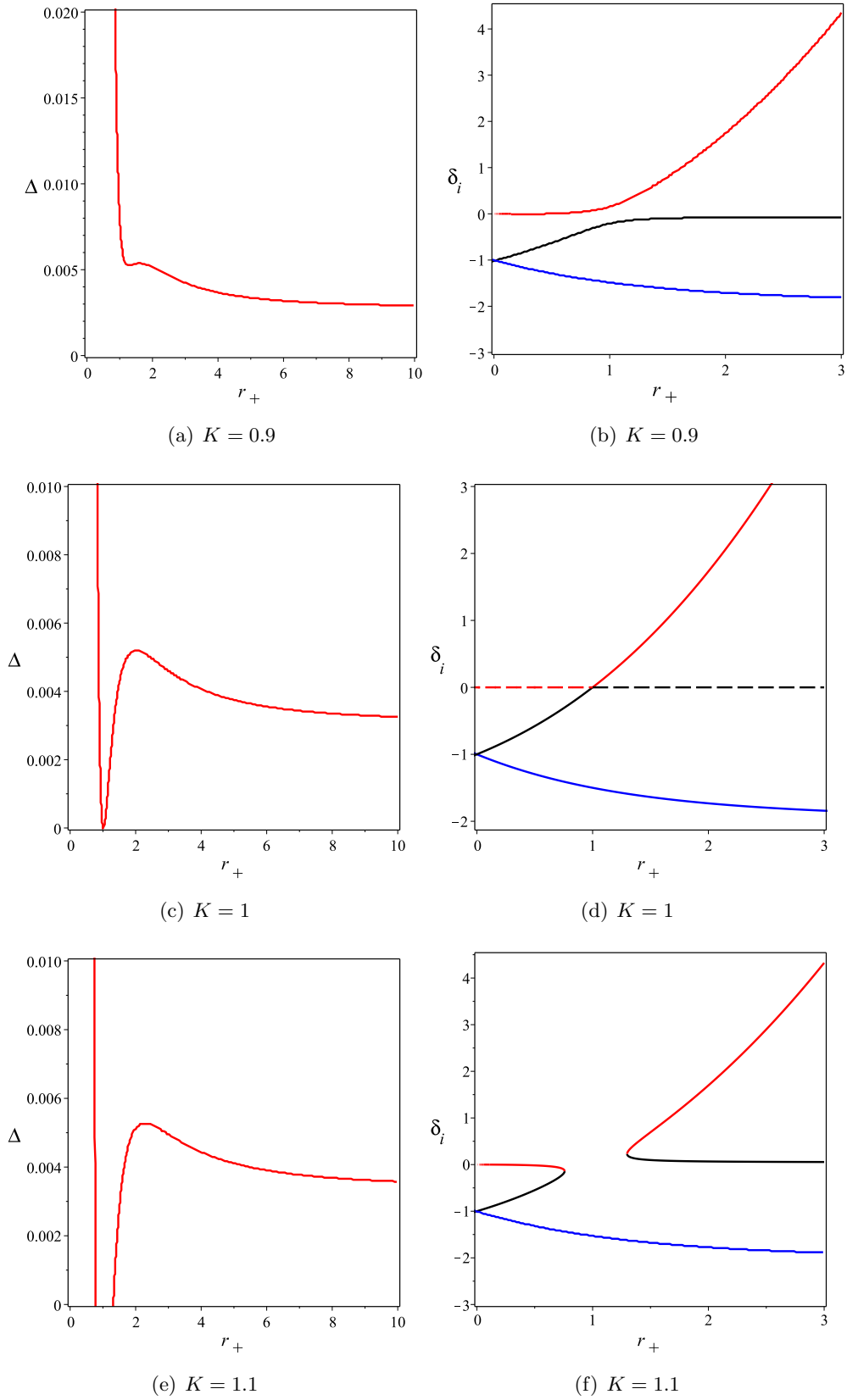


Figure 3: Plots of Δ in terms of r_+ (left) and the behavior of roots (δ_1 (red line), δ_2 (blue line), δ_3 (black line)) in terms of r_+ (right) for $\alpha = 0.5$ and different values of K .

By inserting δ into (27), (28) and (32), we obtain similar behavior for the temperature, entropy and mass of the black hole. In Fig. 4 we illustrate the behavior of M , S and T in terms of r_+ for different values of K . For $K = 1$, the dashed and solid lines correspond to the Schwarzschild and non-Schwarzschild-like behaviour, respectively. For this case the black solid line correspond to the cold non-Schwarzschild black hole while the red solid line correspond to the hot non-Schwarzschild black holes [24].

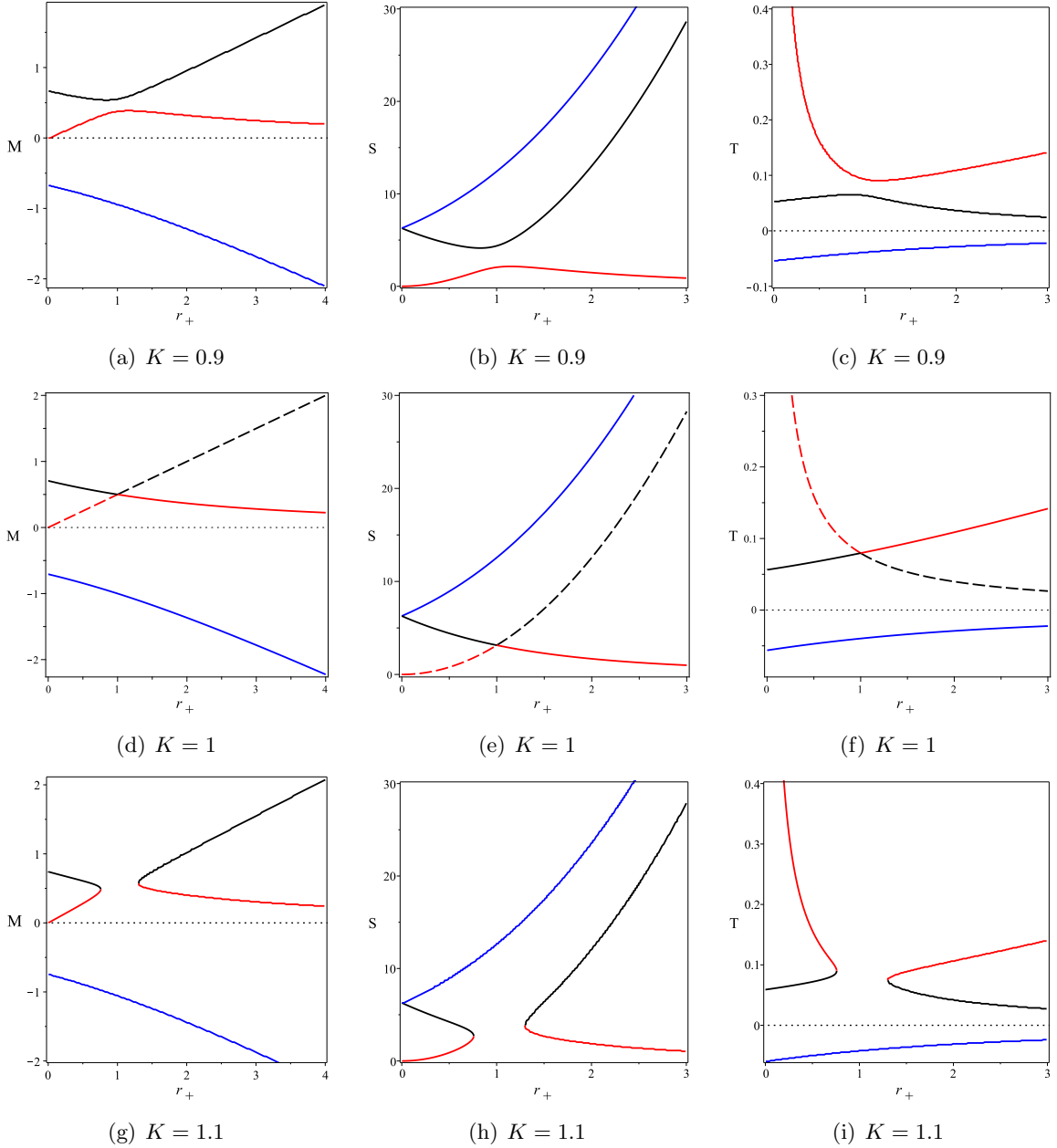


Figure 4: Plots of M , S and T in terms of r_+ for $\alpha = 0.5$ and different values of K . In the middle figures the dashed line curves indicate Schwarzschild-like behaviour and solid line curves non-Schwarzschild-like behaviour. The colors correspond to the colors in figure (3).

In Fig. 5, we will depict the behaviour of S as a function of M and M as a function of T for

the two solutions of δ and different values of K . The third solution of δ doesn't have physical meaning (blue curve). This leads to the negative entropy and mass which we did not show in Fig. 5. For instance, in Fig. 5(c, d) we observe Schwarzschild-like behaviour that starts with the red curve and then smoothly is connected to the orange dotted line. While non-Schwarzschild-like behaviour first follows the black line and then continues with the green dotted line.

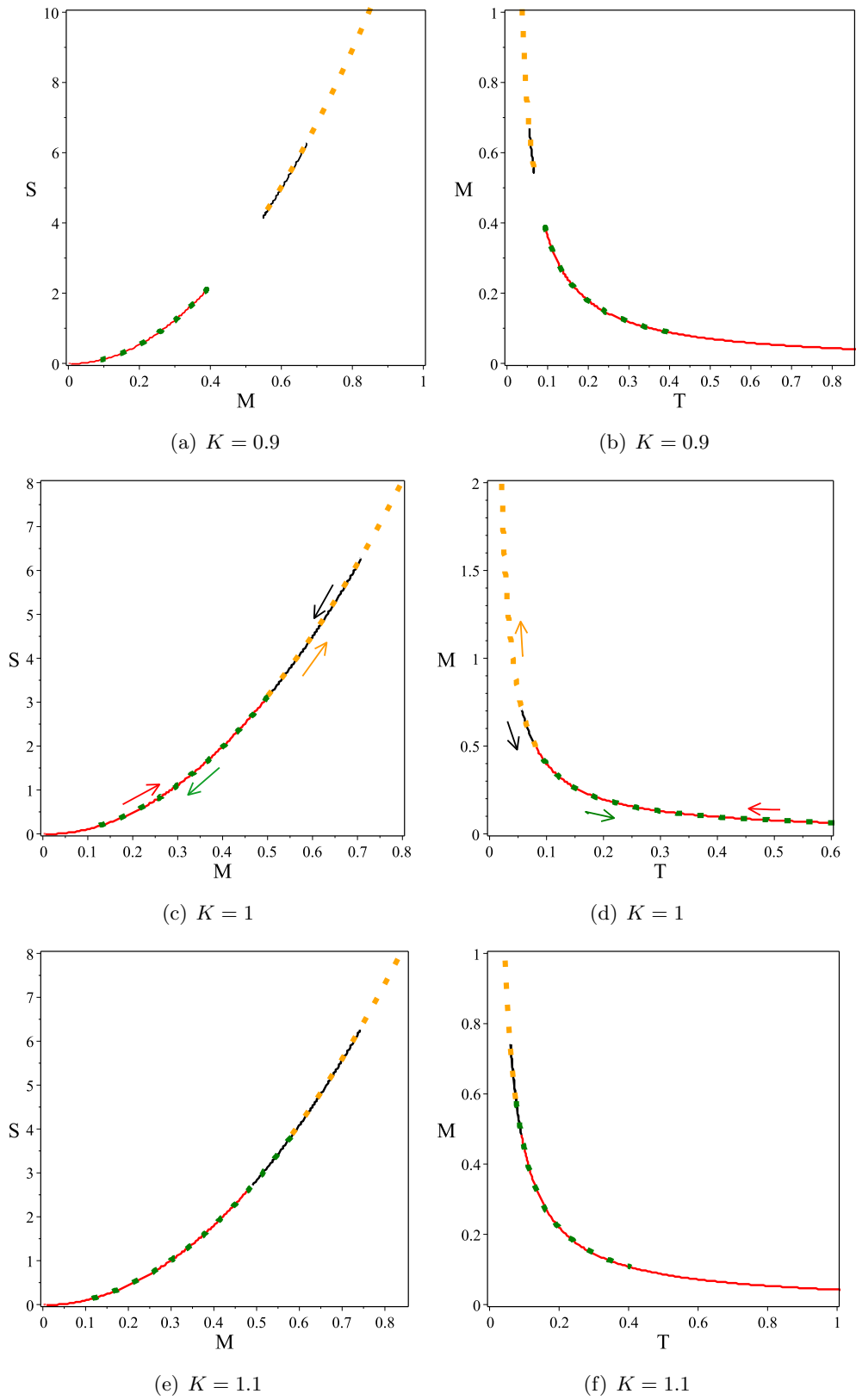


Figure 5: Plots of S in terms of M (left), and of M in terms of T (right) for $\alpha = 0.5$ and different values of K . The direction of the arrows shows the direction of increasing r_+ . Schwarzschild-like behaviour is shown in red and orange.

For $q \neq 0$ we cannot obtain an analytic solution. However we can obtain a solution to leading order in α and q^2 . Expanding $\delta(r_+, q)$ in powers of α we find

$$\delta(r_+, q) = -\frac{q^2}{r_+^2} + \alpha \left(C_1 - \frac{2q^2}{r_+^4} \right) + \dots \quad (42)$$

yielding

$$M = M_0 + \alpha M_1 + \dots = \frac{r_+}{2} + \frac{q^2}{2r_+} + \left(\frac{q^2}{r_+^3} + \frac{C_1 r_+}{2} \right) \alpha + \dots \quad (43)$$

where C_1 is an arbitrary constant of integration with dimension of $1/[length]^2$. We plot in Fig. 2 the quantity $M_1 = (M - M_0)/\alpha$ for different values of C_1 . Obtaining the higher order terms will necessitate obtaining corrections to the potential 29.

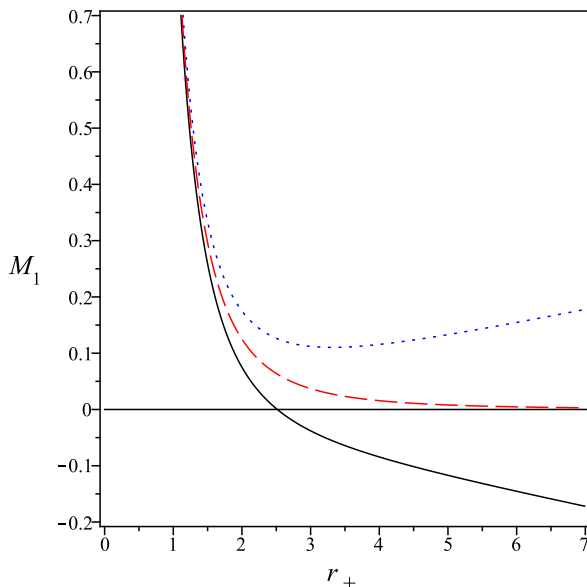


Figure 6: Plots of M_1 in terms of r_+ for $q = 1, C_1 = -0.05$ (solid line), $C_1 = 0$ (red dashed line), $C_1 = 0.05$ (blue dotted line).

3 Particle Orbits in the Schwarzschild-Like Solutions

In this section we examine the behaviour of time-like and null geodesics for these black hole solutions.

Consider the general form of the spherically symmetric line element:

$$ds^2 = -h(r)dt^2 + \frac{dr^2}{f(r)} + r^2 d\theta^2 + r^2 \sin^2(\theta) d\phi^2. \quad (44)$$

Since the metric is independent of t and ϕ , there are two conserved quantities:

$$E = h\dot{t} \quad , \quad L = r^2\dot{\phi}. \quad (45)$$

Without loss of generality we consider the metric on the equatorial plane ($\theta = \frac{\pi}{2}$), and obtain the geodesic equation

$$\frac{1}{2} \frac{h}{f} \dot{r}^2 + \frac{1}{2} \left[h(r) \left(\frac{l^2}{r^2} + 1 \right) \right] = \frac{E^2}{2} \quad (46)$$

for massive neutral particles. The second term is effective potential that we want to study. Note that the kinetic energy term has a non-canonical normalization [19].

We shall work in the asymptotic regime, where the Yukawa terms can be neglected: for $r = 10M, \alpha = 0.5M^2, q = 0.5M$ the respective ratios of the coefficients of the C_2 term in (17) to the second and third terms in (20) are 2.5×10^{-4} and 2×10^{-2} . Eq. (22) then becomes

$$h(r) = 1 - \frac{2M}{r} + \frac{q^2}{r^2} - \left[\frac{128M(1+\delta)}{r^3} - \frac{16q^2(1+\delta)}{r^3 r_+} \right] \alpha, \quad B(x) = 1 \quad (47)$$

yielding $f(r) = h(r)$. So, the effective potential is

$$V_{eff} = \frac{1}{2} \left[h(r) \left(\frac{l^2}{r^2} + 1 \right) \right] = \frac{1}{2} \left(1 - \frac{2M}{r} + \frac{q^2}{r^2} - \left[\frac{128M(1+\delta)}{r^3} - \frac{16q^2(1+\delta)}{r^3 r_+} \right] \alpha \right) \left(\frac{l^2}{r^2} + 1 \right) \quad (48)$$

valid for large r and small α , by using the continued fraction expansion up to order 2. This expansion is not valid to higher orders in the continued fraction expansion, which exhibits terms inversely proportional to α .

In Fig. 7, we plot the approximation to V_{eff} given in (48). We have set $\alpha = 0.5M^2$ and considered different values of L . For large L , there are two extreme points in V_{eff} . The maximum (minimum) point is related to unstable (stable) circular orbits for massive particles.

We can find the ISCO (Innermost Stable Circular Orbit) of the potential in (48) by computing the point of inflection of the effective potential. We find, for example, that for $\alpha = 0.5M^2, q = 0.5M, r_+ = 2M, f_1 = \frac{0.53}{M}, r_{ISCO} = 15.57M$ and $|L_{ISCO}| = 5.33M$ and it is different from the respective Schwarzschild values of $6M$ and $2\sqrt{3}M$ (Fig. 7a). However Fig. 8 indicates that when α goes to zero, r_{ISCO} and $|L_{ISCO}|$ go to $5.6M$ and $3.33M$, respectively. We can also consider a case that would be above extremality in Einstein gravity: $\alpha = 0.5M^2, q = 2M, r_+ = 2M, f_1 = \frac{0.95}{M}$, for which we obtain $r_{ISCO} = 16.07M$ and $|L_{ISCO}| = 5.11M$ (Fig. 7b). Note that $q = 2M$ is not beyond the extremal value for the parameters. Because $q = \sqrt{2}r_+$ is the extremal case while here $q = r_+$.

We find that r_{ISCO} and L_{ISCO} both increase for increasing α , shown in Fig. 8. However, as q increases we find that r_{ISCO} and L_{ISCO} decrease. We illustrate this behaviour in Fig. 9. Also,

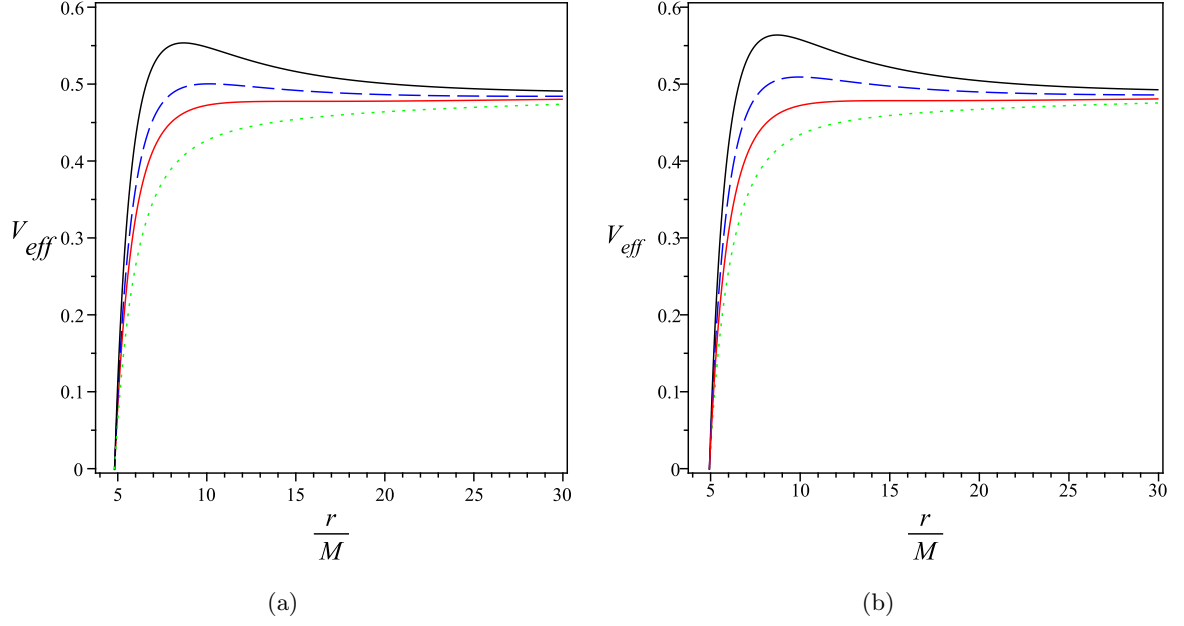


Figure 7: Plots of V_{eff} in terms of $\frac{r}{M}$ for $\alpha = 0.5M^2, k = 1, \Lambda = 0, q = 0.5M, r_+ = 2M, f_1 = \frac{0.53}{M}$ and $\frac{L}{M} = 4, 5.33, 6, 7$ from (green dotted line) to (black solid line)(left), and for $\alpha = 0.5M^2, k = 1, \Lambda = 0, q = 2M, r_+ = 2M, f_1 = \frac{0.95}{M}$ and $\frac{L}{M} = 4, 5.11, 6, 7$ from (green dashed line) to (black solid line)(right).

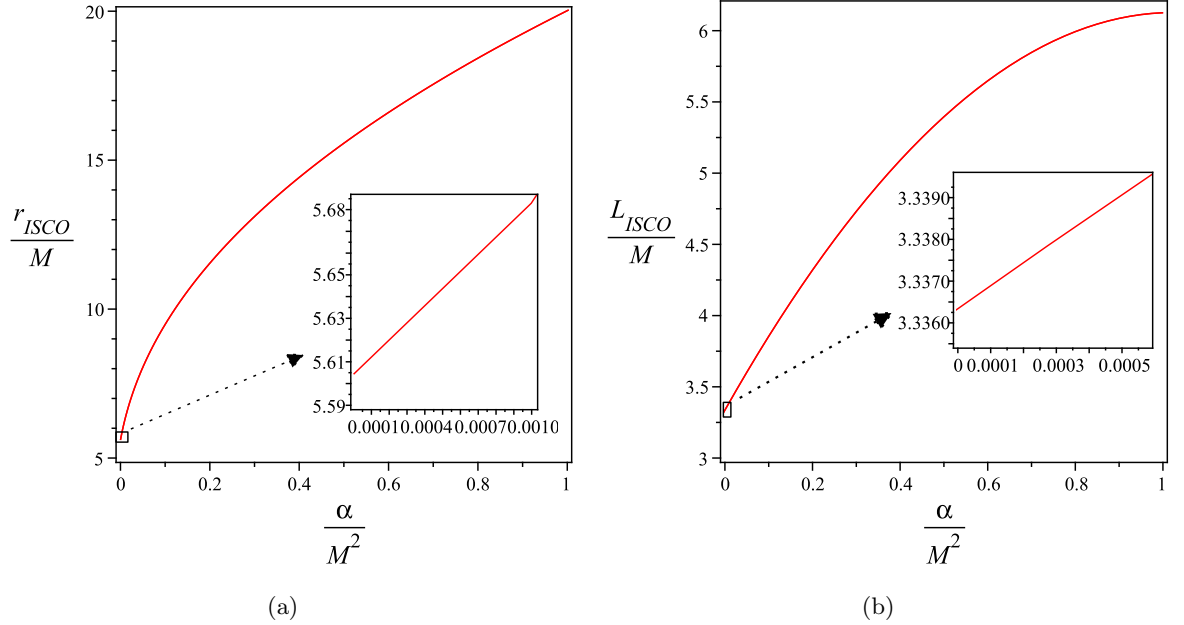


Figure 8: The innermost stable circular orbit (left) and the angular momentum of inflection point (right) in terms of the coupling constant of theory ($\frac{\alpha}{M^2}$) for $k = 1, \Lambda = 0, q = 0.5M, r_+ = 2M, f_1 = \frac{0.53}{M}$.

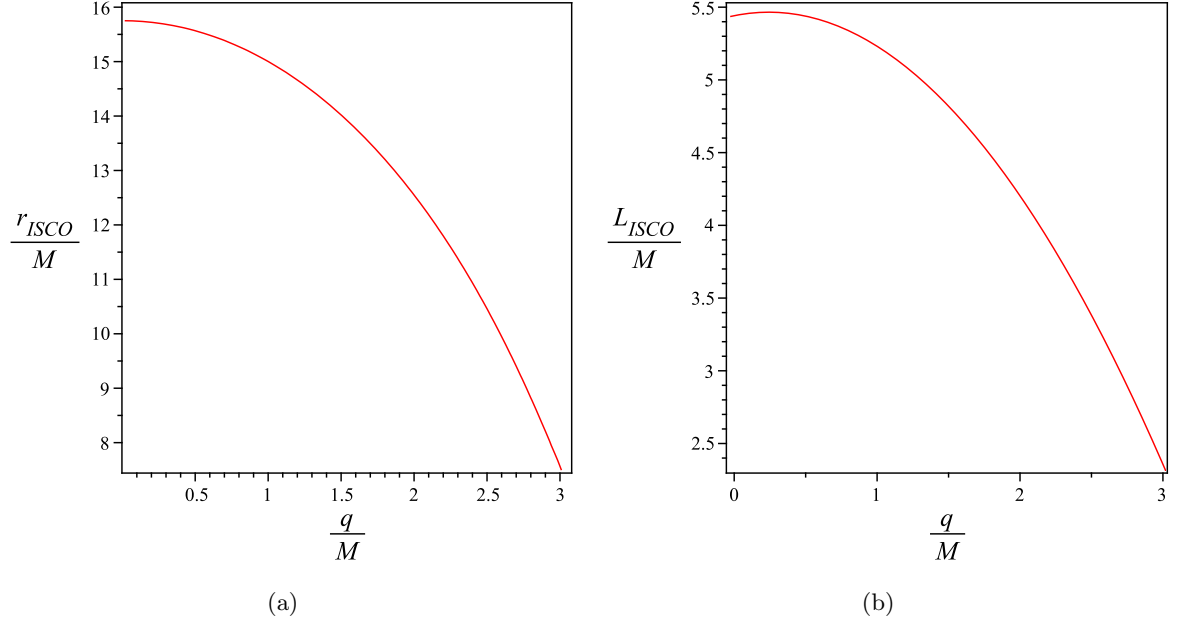


Figure 9: The innermost stable circular orbit (left) and the angular momentum of inflection point (right) in terms of electric charge ($\frac{q}{M}$) for $k = 1, \Lambda = 0, \alpha = 0.5M^2, r_+ = 2M, f_1 = \frac{0.53}{M}$.

We now turn to a consideration of the behaviour of null geodesics in the vicinity of the black hole. The deflection of the photon as it moves from infinity to r_m and off to infinity for the metric (4) can be expressed as

$$\delta\varphi = \int_{r_m}^{\infty} \frac{2dr}{\sqrt{\frac{f}{h} \frac{r^4}{b^2} - fr^2}} - \pi = I - \pi, \quad (49)$$

where $b = \sqrt{\frac{r_m^2}{h(r_m)}}$ is the impact parameter of the null ray and r_m is coordinate distance of closest approach. Here π is the change in the angle φ for straight line motion and is therefore subtracted out. In the asymptotic regime (up to 2nd order (a_2 and b_2) in the continued fraction expansion) with $q = 0$ we have

$$f(r) \approx h(r) \approx 1 - \frac{2M}{r} - \frac{128M(1+\delta)\alpha}{r^3}, \quad B \approx 1 \quad (50)$$

We now calculate the integral in (49) using (50). Writing the term in the denominator of (49) as $h(r)r^2 (r^2/b^2h(r) - 1)$, we have

$$\begin{aligned} \frac{h(r_m)}{h(r)} \frac{r^2}{r_m^2} - 1 &= \left[\frac{1 - \frac{2M}{r_m} - \frac{128M\alpha(1+\delta)}{r_m^3}}{1 - \frac{2M}{r} - \frac{128M\alpha(1+\delta)}{r^3}} \right] \left(\frac{r^2}{r_m^2} \right) - 1 = \\ &= \left(\frac{r}{r_m} \right)^2 \left[1 + 2M \left(\frac{1}{r} - \frac{1}{r_m} \right) + 128M\alpha(1+\delta) \left(\frac{1}{r^3} - \frac{1}{r_m^3} \right) \right] - 1 = \\ &= \left(\frac{r^2}{r_m^2} - 1 \right) \left[1 - \frac{2Mr}{r_m(r+r_m)} - \frac{128M\alpha(1+\delta)}{rr_m^2} \left(1 + \frac{r^2}{r_m(r+r_m)} \right) \right] \quad (51) \end{aligned}$$

for $M \ll r$. The integrand becomes

$$\int_{r_m}^{\infty} \frac{1}{\sqrt{\left(\frac{1}{r_m^2} - \frac{1}{r^2}\right)}} \left[1 + \frac{M}{r} \left(1 + \frac{r^2}{r_m(r+r_m)} \right) + \frac{64M\alpha(1+\delta)}{r^3} \left(1 + \frac{r^2}{r_m^2} \left(1 + \frac{r^2}{r_m(r+r_m)} \right) \right) \right] \frac{dr}{r^2} \quad (52)$$

upon expanding in powers of M/r , M/r_m , and α/M^2 .

After making the substitution $\sin(\theta) = \frac{r_m}{r}$ the integral becomes

$$\int_0^{\frac{\pi}{2}} d\theta \left[1 + \frac{M}{r_m} \left(\sin(\theta) + \frac{1}{1+\sin(\theta)} \right) + \frac{64M\alpha(1+\delta)}{r_m^3} \left(\sin^3(\theta) + \sin(\theta) + \frac{1}{1+\sin(\theta)} \right) \right] = \frac{\pi}{2} + \frac{2M}{r_m} + \frac{512M\alpha(1+\delta)}{3r_m^3} \quad (53)$$

The deflection is as follows

$$\Delta\varphi = \frac{4M}{r_m} + \frac{1024M\alpha(1+\delta)}{3r_m^3} \quad (54)$$

valid for large r ($r \rightarrow \infty$) and small α ($\alpha \rightarrow 0$), where δ is given in (27). So, above is a simple modification of the standard Einstein result of $4M/r_m$. The constant α must be small enough such that the extra term is negligible compared to $4M/r_m$ on solar system distance scales.

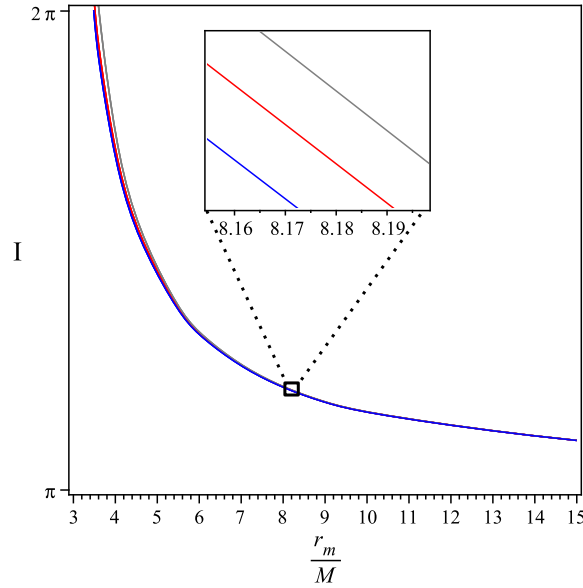


Figure 10: Plots of deflection angle in terms of r_m for $k = 1, \Lambda = 0, q = 0.5M, r_+ = 2M, f_1 = \frac{0.53}{M}$ and $\alpha = 0.05M^2, 0.5M^2, M^2$ from (gray dashed line) to (blue solid line).

In Fig. 10, we plot the deflection angle in terms of closest distance to the black hole. As r_m increases the deflection angle decreases and goes to π . However we see that as α increases the

deflection angle diverges at smaller values of r_m relative to the Schwarzschild case, we see that deflection angle diverges at $r_m = 3.5M$ as α/M^2 approaches unity. The location at which the deflection angle diverges is the radius of the photon sphere.

We next consider the shadow of these black holes. In fact, we follow up the null geodesics which satisfy the condition $R'' > 0$, i.e, unstable circular orbits. The angular radius of the shadow as seen by an observer at r_0 is [22]

$$\sin^2(\Gamma) = \frac{r_{ph}^2 h(r_0)}{r_0^2 h(r_{ph})} \quad (55)$$

and using of Eq. (47) for $h(r)$ with $q = 0$ we obtain

$$\begin{aligned} \frac{r_{ph}^2 f(r_0)}{r_0^2 f(r_{ph})} &= \frac{r_{ph}^2}{r_0^2} \left[\frac{1 - \frac{2M}{r_0} - \frac{128M\alpha(1+\delta)}{r_0^3}}{1 - \frac{2M}{r_{ph}} - \frac{128M\alpha(1+\delta)}{r_{ph}^3}} \right] \\ &= \frac{r_p^2}{r_0^2} \left[\left(1 - \frac{2M}{r_0} - \frac{128M\alpha(1+\delta)}{r_0^3} \right) \left(1 + \frac{2M}{r_{ph}} + \frac{128M\alpha(1+\delta)}{r_{ph}^3} \right) \right] \\ &= \frac{r_p^2}{r_0^2} \left[1 + 2M \left(\frac{1}{r_{ph}} - \frac{1}{r_0} \right) + 128M\alpha(1+\delta) \left(\frac{1}{r_{ph}^3} - \frac{1}{r_0^3} \right) \right] \end{aligned} \quad (56)$$

yielding in turn

$$\sin(\Gamma) = \frac{r_{ph}}{r_0} + \frac{M(r_0 - r_{ph})}{r_0^2} + \frac{64M\alpha(1+\delta)(r_0^3 - r_{ph}^3)}{r_{ph}^2 r_0^4} \quad (57)$$

where r_{ph} is the radius of the photon sphere and Γ is the angle subtended by the radius of the shadow as seen by an observer at r_0 .

In the case of small Γ , we have $\sin(\Gamma) \approx \Gamma$, so

$$\Gamma = \Gamma_{Ein} + \Gamma_{Con} \quad (58)$$

up to 2nd order in the continued fraction expansion, i.e. the asymptotic regime. In above equation on the right hand side, the first two term are the Einstein term and the second term the correction from the Quadratic corrections.

Finally, we consider Shapiro time-delay to obtain a bound on the coupling constant α . The general expression for time delay for the metric (44) is

$$t(r_0, r) = \int_{r_0}^r \frac{dr}{\sqrt{f(r)h(r) \left(1 - \frac{r_0^2 h(r)}{r^2 h(r_0)} \right)}} \quad (59)$$

In order to evaluate the integral, we expand the metric at asymptotic regime as in (50). Similar manipulations as before yield

$$\frac{1}{\sqrt{1 - \frac{r_0^2}{r^2}}} \left(1 + \frac{M}{r} \left(1 + \frac{r_0}{(r+r_0)} \right) + \frac{64M(1+\delta)\alpha}{r^3} \left(2 + \frac{r^2}{(r+r_0)r_0} \right) \right) \quad (60)$$

for the integrand. Now, integral is elementary and we find that the time required for light to go from r_0 to r is

$$t(r, r_0) \approx \sqrt{r^2 - r_0^2} + M \ln \left(\frac{r + \sqrt{r^2 - r_0^2}}{r_0} \right) + M \sqrt{\frac{r - r_0}{r + r_0}} + \frac{M(1 + \delta)\alpha}{r_0} \sqrt{\frac{r - r_0}{r + r_0}} \left(\frac{192}{r_0} + \frac{128}{r} \right) \quad (61)$$

Working in the asymptotic regime (to 2nd order in the continued fraction expansion) schematically this expression is

$$t(r, r_0) = t_{SR}(r, r_0) + \Delta t_{GR}(r, r_0) + \Delta t_{EC}(r, r_0) = t_{SR}(r, r_0) + \Delta t(r, r_0) \quad (62)$$

where $t_{SR} = \sqrt{r^2 - r_0^2}$ is the special relativistic contribution of the propagation of light in flat spacetime. So, the maximum round-trip excess time delay is given by

$$\begin{aligned} \Delta t(r, r_0) &= 2 \left[t(r_2, r_0) + t(r_1, r_0) - \sqrt{r_1^2 - r_0^2} - \sqrt{r_2^2 - r_0^2} \right] = 2M \ln \left[\frac{(r_1 + \sqrt{r_1^2 - r_0^2})(r_2 + \sqrt{r_2^2 - r_0^2})}{r_0^2} \right] \\ &+ 2M \left[\sqrt{\frac{r_1 - r_0}{r_1 + r_0}} + \sqrt{\frac{r_2 - r_0}{r_2 + r_0}} \right] + \frac{2M\alpha(1 + \delta)}{r_0} \left[\sqrt{\frac{r_1 - r_0}{r_1 + r_0}} \left(\frac{192}{r_0} + \frac{128}{r_1} \right) + \sqrt{\frac{r_2 - r_0}{r_2 + r_0}} \left(\frac{192}{r_0} + \frac{128}{r_2} \right) \right] \end{aligned} \quad (63)$$

in the case of $r_1 = r_2 = r$, this becomes

$$\Delta t(r, r_0) = 4M \ln \left(\frac{r + \sqrt{r^2 - r_0^2}}{r_0} \right) + 4M \sqrt{\frac{r - r_0}{r + r_0}} + \frac{4\alpha(1 + \delta)}{M^2} \sqrt{\frac{r - r_0}{r + r_0}} \left(\frac{192M^3}{r_0^2} + \frac{128M^3}{rr_0} \right) \quad (64)$$

where we have partitioned the expression into the general relativistic (GR) and Einstein-Conformal (EC) corrections. Here r_0 is the distance of closest approach of the radar wave to the center of the Sun, r_1 is the distance along the line of light from the Earth to the point of closest approach to the Sun, and r_2 represents the distance along the path from this point to the planet, where $r_{1,2} \gg r_0$.

Taking the smallest possible value of r as the radius of the sun $r_\odot = 6.957 \times 10^8$ m, we see that the coefficient of the Einstein conformal correction is about $(M_\odot/r_\odot)^2 \sim 4.5 \times 10^{-12}$, where $M = M_\odot = 1477$ m, implying that $\alpha(1 + \delta)/M^2$ need not be extremely small. Deviations of time delay from the prediction of general relativity have been constrained to be less than 0.000012 [15], and so the last term in (64) must be no larger than this value [12]- [15]. Using solar system data (where in units of metres, $r_1 = r_2 = 10^{11}$ m, $r_0 = r_\odot = 10^8$ m), we obtain the constraint

$$\frac{\alpha(1 + \delta)}{M_\odot^2} < 0.05. \quad (65)$$

We note by comparison recent work [23] making use of exoplanet data to constrain modifications of the form $\tilde{\alpha}^{(N)}/r^N$ to the effective gravitational potential in the weak-field limit. For the theory we are considering, $N = 3$, but $\tilde{\alpha}^{(N)} = \alpha(1 + \delta)M$ from (48), so the appropriate parameter to compare to is $\tilde{\alpha}^{(2)}$ because of the mass parameter. Inserting units into the bound in (65), we find

$$\alpha(1 + \delta) < 0.05 \left(\frac{GM_\odot}{c^2} \right)^2 c^2 \sim 9.8 \times 10^{21} \text{ m}^4/\text{s}^2 \quad (66)$$

comparable to the limit $\tilde{\alpha}^{(2)} < 10^{22} \text{ m}^4/\text{s}^2$ obtained from exoplanet data.

4 Conclusion

We have obtained an analytic approximation to a charged black hole solutions in Einstein Quadratic gravity by making use of a continued fraction expansion. The key advantage to this approach is that the continued fraction can be used in place of an exact solution, allowing one to study problems that are difficult to address by numeric methods. We have studied thermodynamics of the black hole in the absence of cosmological constant. Working to leading order in α and q^2 , we have shown the first law and Smarr formula is satisfied.

We also investigated phenomenological consequences of the $q = 0$ solution. We found that for a given value of the mass, the ISCO for a massive test body, as well as its angular momentum at that location grows as the parameter α increases.

We note that our approximations need to be taken with care. As for the $q = 0$ case [5], the near-horizon expansions (9) and (10) of the metric functions do not have a sensible small- α limit. Beyond 2nd order in the continued fraction expansion the same thing happens. This means that the small- α expansions must be understood as asymptotic expansions, and should not be taken to apply in the strong-field limit.

This raises the question as to whether or not the solution presented in section 2 is an appropriate generalization of the Schwarzschild solution. We present in Appendix B an alternate near horizon solution with a well-defined $\alpha \rightarrow 0$ limit, analogous to that obtained in Einstein Cubic gravity [15]. Exploring the physical consequences of this solution remains an interesting subject for future study.

Acknowledgements

This work was supported in part by the Natural Sciences and Engineering Research Council of Canada.

A Explicit Terms in the Continued Fraction Approximation

We present terms up to order 4 in the continued fraction approximation (25):

$$\begin{aligned}
 \epsilon &= -\frac{F_1}{r_+} - 1, \quad a_1 = -1 - a_0 + 2\epsilon + r_+ h_1, \quad a_2 = -\frac{4a_1 - 5\epsilon + 1 + 3a_0 + h_2 r_+^2}{a_1} \\
 a_3 &= -\frac{1}{a_1 a_2} [-h_3 r_+^3 + a_1 a_2^2 + 5a_1 a_2 + 6a_0 + 10a_1 - 9\epsilon + 1] \\
 a_4 &= -\frac{h_4 r_+^4 + a_1 a_2^3 + 2a_1 a_2^2 a_3 + a_1 a_2 a_3^2 + 6a_1 a_2^2 + 6a_1 a_2 a_3 + 15a_1 a_2 + 10a_0 + 20a_1 - 14\epsilon + 1}{a_1 a_2 a_3}
 \end{aligned} \tag{67}$$

and

$$\begin{aligned}
b_1^\pm &= -1 \pm \sqrt{\frac{h_1}{f_1}}, \quad b_2 = -\frac{r_+(f_1 h_2 - f_2 h_1)(b_1 + 1) + 4b_1 f_1 h_1}{2b_1 f_1 h_1}, \\
b_3 &= -\frac{1}{f_1^2 h_1^2} [-4f_1^2 h_1 h_3 r_+^2 b_1 - 4f_1^2 h_1 h_3 r_+^2 + f_1^2 h_2^2 r_+^2 b_1 + f_1^2 h_2^2 r_+^2 + 2f_1 f_2 h_1 h_2 r_+^2 b_1 \\
&\quad + 2f_1 f_2 h_1 h_2 r_+^2 + 4f_1 f_3 h_1^2 r_+^2 b_1 + 4f_1 f_3 h_1^2 r_+^2 - 3f_2^2 h_1^2 r_+^2 b_1 - 3f_2^2 h_1^2 r_+^2 \\
&\quad + 8b_1 b_2^2 f_1^2 h_1^2 + 24b_1 b_2 f_1^2 h_1^2 + 24b_1 f_1^2 h_1^2] \quad (68) \\
b_4 &= -\frac{1}{16b_1 b_2 b_3 f_1^3 h_1^3} [96b_1 b_2 f_1^3 h_1^3 + 64b_1 f_1^3 h_1^3 + 64b_1 b_2^2 f_1^3 h_1^3 + 32b_1 b_2^2 b_3 f_1^3 h_1^3 + \\
&\quad 16b_1 b_2 b_3^2 f_1^3 h_1^3 + 64b_1 b_2 b_3 f_1^3 h_1^3 + 16b_1 b_2^3 f_1^3 h_1^3 + f_1^3 h_2^3 r_+^3 + f_1^3 h_2^3 r_+^3 b_1 - 5f_2^3 h_1^3 r_+^3 \\
&\quad - 5f_2^3 h_1^3 r_+^3 b_1 + 8f_1^3 h_1^2 h_4 r_+^3 + 8f_1^3 h_1^2 h_4 r_+^3 b_1 - 4f_1^3 h_1 h_2 h_3 r_+^3 - 4f_1^3 h_1 h_2 h_3 r_+^3 b_1 \\
&\quad - 4f_1^2 f_2 h_1^2 h_3 r_+^3 - 4f_1^2 f_2 h_1^2 h_3 r_+^3 b_1 + f_1^2 f_2 h_1 h_2^2 r_+^3 + f_1^2 f_2 h_1 h_2^2 r_+^3 b_1 - 4f_1^2 f_3 h_1^2 h_2 r_+^3 \\
&\quad - 4f_1^2 f_3 h_1^2 h_2 r_+^3 b_1 - 8f_1^2 f_4 h_1^3 r_+^3 - 8f_1^2 f_4 h_1^3 r_+^3 b_1 + 3f_1 f_2^2 h_1^2 h_2 r_+^3 + 3f_1 f_2^2 h_1^2 h_2 r_+^3 b_1 \\
&\quad + 12f_1 f_2 f_3 h_1^3 r_+^3 + 12f_1 f_2 f_3 h_1^3 r_+^3 b_1]
\end{aligned}$$

The quantities f_2 and h_2 are respectively given in (9) and (10) and

$$\begin{aligned}
f_3 &= \frac{-30q^2 f_1 h_2 - 180\alpha k f_1^3 + 336\alpha r_+ f_1^4 + 60kr_+ f_1^2 - 30r_+^3 f_2 f_1^2 - 120r_+^3 f_1^2 h_2 + 120\Lambda r_+^3 f_1^2}{\alpha r_+^3 f_1^3} - \\
&\quad \frac{15q^2 f_2 f_1 - 728\Lambda \alpha r_+^2 f_1^3 - 204\alpha k r_+ f_1^2 h_2 - 728\Lambda \alpha r_+^3 f_1^2 h_2 - 120r_+^2 f_1^3 + 507\alpha r_+^2 f_1^3 f_2}{\alpha r_+^3 f_1^3} + \\
&\quad \frac{75\alpha r_+^3 f_2^2 f_1^2 + 90kr_+^2 f_1 h_2 + 513\alpha r_+^2 f_1^3 h_2 + 90\Lambda r_+^4 f_1 h_2 - 54\alpha r_+^3 f_1^2 h_2^2 - 120\alpha k r_+ f_2 f_1^2}{\alpha r_+^3 f_1^3} - \\
&\quad \frac{320\Lambda \alpha r_+^3 f_2 f_1^2 + 320\Lambda^2 \alpha r_+^3 f_1^2 + 160\Lambda \alpha k r_+ f_1^2 + 240\Lambda \alpha k r_+^2 f_1 h_2 + 240\Lambda^2 \alpha r_+^4 f_1 h_2 + 303\alpha r_+^3 f_1^2 f_2 h_2}{\alpha r_+^3 f_1^3} \\
h_3 &= \frac{-6q^2 f_1 h_2 - 36\alpha k f_1^3 - 192\alpha r_+ f_1^4 + 12kr_+ f_1^2 - 6r_+^3 f_2 f_1^2 - 24r_+^3 f_1^2 h_2 + 24\Lambda r_+^3 f_1^2}{216\alpha r_+^3 f_1^3} - \\
&\quad \frac{3q^2 f_2 f_1 + 200\Lambda \alpha r_+^2 f_1^3 + 132\alpha k r_+ f_1^2 h_2 + 200\Lambda \alpha r_+^3 f_1^2 h_2 - 24r_+^2 f_1^3 - 201\alpha r_+^2 f_1^3 f_2 + 15\alpha r_+^3 f_2^2 f_1^2}{216\alpha r_+^3 f_1^3} + \\
&\quad \frac{18kr_+^2 f_1 h_2 - 459\alpha r_+^2 f_1^3 h_2 + 18\Lambda r_+^4 f_1 h_2 - 54\alpha r_+^3 f_1^2 h_2^2 - 24\alpha k r_+ f_2 f_1^2 - 64\Lambda \alpha r_+^3 f_2 f_1^2}{216\alpha r_+^3 f_1^3} + \\
&\quad \frac{64\Lambda^2 \alpha r_+^3 f_1^2 + 32\Lambda \alpha k r_+ f_1^2 + 48\Lambda \alpha k r_+^2 f_1 h_2 + 48\Lambda^2 \alpha r_+^4 f_1 h_2 - 69\alpha r_+^3 f_1^2 f_2 h_2}{216\alpha r_+^3 f_1^3}
\end{aligned}$$

B An alternate Near-horizon Solution

An alternate near horizon solution with a well-defined $\alpha \rightarrow 0$ limit can be obtained by taking r_+ and h_2 to be the undetermined constants of integration. This yields

$$f_1 = \frac{1}{96r_+^2(r_+h_2 + 2h_1)\alpha} [80\Lambda\alpha r_+^3 h_1 + 48\alpha k r_+ h_1 - 6r_+^3 h_1 - 3q^2 + (3072\Lambda^2\alpha^2 r_+^7 h_1 h_2 + 12544\Lambda^2\alpha^2 r_+^6 h_1^2 + 3072\Lambda\alpha^2 k r_+^5 h_1 h_2 + 1152\Lambda\alpha r_+^7 h_1 h_2 + 13824\Lambda\alpha^2 k r_+^4 h_1^2 + 1344\Lambda\alpha r_+^6 h_1^2 + 1152\alpha k r_+^5 h_1 h_2 + 13824\Lambda\alpha^2 k r_+^4 h_1^2 + 1344\Lambda\alpha r_+^4 h_1^2 + 1152\alpha k r_+^5 h_1 h_2 - 480\Lambda\alpha q^2 r_+^3 h_1 + 2304\alpha k^2 r_+^2 h_1^2 + 1728\alpha k r_+^4 h_1^2 + 36r_+^4 h_1^2 - 288\alpha k q^2 r_+ h_1 + 36q^2 r_+^3 h_1 + 9q^4)^{\frac{1}{2}}] \quad (69)$$

and

$$f_2 = \frac{1}{h_1 r_+^2} [-3f_1 h_2 r_+^2 - 8f_1 h_1 r_+ + 4k h_1 + 8\Lambda h_1 r_+^2] \quad (70)$$

$$f_3 = \frac{1}{r_+^2 h_1} [8\Lambda r_+^2 h_1 h_2 - 5r_+^2 f_1 h_1 h_3 - r_+^2 f_1 h_2^2 - 3r_+^2 f_2 h_1 h_2 + 8\Lambda r_+ h_1^2 - 13r_+ f_1 h_1 h_2 - 7r_+ f_2 h_1^2 + 4k h_1 h_2 - 6f_1 h_1^2]$$

$$h_3 = \frac{1}{216h_1\alpha r_+^3 f_1^2} [48\Lambda^2\alpha r_+^4 h_1 h_2 + 64\Lambda^2\alpha r_+^3 h_1 + 200\Lambda\alpha r_+^3 f_1 h_1 h_2 - 64\Lambda\alpha r_+^3 f_2 f_1^2 - 54\alpha r_+^3 f_1^2 h_2^2 - 69\alpha r_+^3 f_1 f_2 h_1 h_2 + 15\alpha r_+^3 f_2^2 h_1^2 + 48\Lambda\alpha k r_+^2 h_1 h_2 + 200\Lambda\alpha r_+^2 f_1 h_1^2 + 18\Lambda r_+^4 h_1 h_2 - 459\alpha r_+^2 f_1^2 h_1 h_2 - 201\alpha r_+^2 f_1 f_2 h_1^2 + 32\Lambda\alpha k r_+ h_1^2 + 24\Lambda r_+^3 h_1^2 + 132\alpha k r_+ f_1 h_1 h_2 - 24\alpha k r_+ f_2 h_1^2 - 192\alpha r_+ f_1^2 h_1^2 - 24r_+^3 f_1 h_1 h_2 - 6r_+^3 f_2 h_1^2 - 36\alpha k f_1 h_1^2 + 18k r_+^2 h_1 h_2 - 24r_+^2 f_1 h_1^2 + 12k r_+ h_1^2 - 6q^2 f_1 h_2 - 3q^2 f_2 h_1]$$

The small α limit is

$$f_1 = \frac{2r_+^3 h_1 (\Lambda r_+^2 + k)}{2r_+^3 h_1 + q^2} + \mathcal{O}(\alpha) \quad (71)$$

$$f_2 = \frac{2(-3\Lambda r_+^6 h_2 - 3k r_+^4 h_2 + 4\Lambda q^2 r_+^2 - 4k r_+^3 h_1 + 2k q^2)}{r_+^2 (2r_+^3 h_1 + q^2)} + \mathcal{O}(\alpha) \quad (72)$$

with more complicated expressions for f_3 and h_3 that we shall not write down here. As we are interested in the charged generalization of the black hole solutions obtained in (1), we shall postpone investigation of this alternate solution for future study.

References

- [1] G. 't Hooft and M. J. G. Veltman, Ann. Inst. H. Poincare Phys. Theor. A **20**, 69 (1974).
- [2] K. S. Stelle, Phys. Rev. D **16**, 953 (1977). doi:10.1103/PhysRevD.16.953
- [3] A. V. Smilga, J. Phys. A **47**, no. 5, 052001 (2014) doi:10.1088/1751-8113/47/5/052001 [arXiv:1306.6066 [hep-th]].
- [4] A. V. Smilga, Nucl. Phys. B **706**, 598 (2005) doi:10.1016/j.nuclphysb.2004.10.037 [hep-th/0407231].

- [5] H. Lu, A. Perkins, C. N. Pope and K. S. Stelle, *Phys. Rev. Lett.* **114**, no. 17, 171601 (2015) doi:10.1103/PhysRevLett.114.171601 [arXiv:1502.01028 [hep-th]].
- [6] K. Lin, A. B. Pavan, G. Flores-Hidalgo and E. Abdalla, *Braz. J. Phys.* **47**, no. 4, 419 (2017) doi:10.1007/s13538-017-0505-0 [arXiv:1605.04562 [gr-qc]].
- [7] L. Rezzolla and A. Zhidenko, *Phys. Rev. D* **90**, no. 8, 084009 (2014) doi:10.1103/PhysRevD.90.084009 [arXiv:1407.3086 [gr-qc]].
- [8] E. W. Leaver, *Proc. Roy. Soc. Lond. A* **402**, 285 (1985). doi:10.1098/rspa.1985.0119
- [9] S. Deser and B. Tekin, *Phys. Rev. Lett.* **89**, 101101 (2002) doi:10.1103/PhysRevLett.89.101101 [hep-th/0205318].
- [10] E. Altas and B. Tekin, *Phys. Rev. D* **99**, no. 4, 044016 (2019) doi:10.1103/PhysRevD.99.044016 [arXiv:1811.11525 [hep-th]].
- [11] L. Rezzolla and A. Zhidenko, *Phys. Rev. D* **90**, no. 8, 084009 (2014) doi:10.1103/PhysRevD.90.084009 [arXiv:1407.3086 [gr-qc]].
- [12] A. Edery and M. B. Paranjape, *Phys. Rev. D* **58**, 024011 (1998) doi:10.1103/PhysRevD.58.024011 [astro-ph/9708233].
- [13] H. Asada, *Phys. Lett. B* **661**, 78 (2008) doi:10.1016/j.physletb.2008.02.006 [arXiv:0710.0477 [gr-qc]].
- [14] C. M. Will, *Living Rev. Rel.* **17**, 4 (2014) doi:10.12942/lrr-2014-4 [arXiv:1403.7377 [gr-qc]].
- [15] R. A. Hennigar, M. B. J. Poshteh and R. B. Mann, *Phys. Rev. D* **97**, no. 6, 064041 (2018) doi:10.1103/PhysRevD.97.064041 [arXiv:1801.03223 [gr-qc]].
- [16] R. M. Wald, *Phys. Rev. D* **48**, no. 8, R3427 (1993) doi:10.1103/PhysRevD.48.R3427 [gr-qc/9307038].
- [17] V. Iyer and R. M. Wald, *Phys. Rev. D* **50**, 846 (1994) doi:10.1103/PhysRevD.50.846 [gr-qc/9403028].
- [18] H. Lü, A. Perkins, C. N. Pope and K. S. Stelle, *Phys. Rev. D* **92**, no. 12, 124019 (2015) doi:10.1103/PhysRevD.92.124019 [arXiv:1508.00010 [hep-th]].
- [19] H. Fuchs *Astron. Nach.* **311**, 271 (1990).
- [20] J. G. Cramer, R. L. Forward, M. S. Morris, M. Visser, G. Benford and G. A. Landis, *Phys. Rev. D* **51**, 3117 (1995) doi:10.1103/PhysRevD.51.3117 [astro-ph/9409051].
- [21] D. F. Torres, G. E. Romero and L. A. Anchordoqui, *Phys. Rev. D* **58**, 123001 (1998) doi:10.1103/PhysRevD.58.123001 [astro-ph/9802106].
- [22] J. L. Synge, *Mon. Not. R. astr. Soc.* 131 (1966).
- [23] M. L. Ruggiero and L. Iorio, arXiv:2001.04122 [gr-qc].
- [24] A. Bonanno and S. Silveravalle, *Phys. Rev. D* **99**, no.10, 101501 (2019) doi:10.1103/PhysRevD.99.101501 [arXiv:1903.08759 [gr-qc]].